Anomalously high thermal conductivity of amorphous Si deposited by hot-wire chemical vapor deposition

Ho-Soon Yang
Department of Physics, Pusan National University, Pusan 609-735, Korea

David G. Cahill*
Department of Materials Science and Engineering, and Materials Research Laboratory, University of Illinois, Urbana, Illinois 61801, USA

X. Liu
Naval Research Laboratory, Washington, DC 20375, USA

J. L. Feldman
Center for Computational Materials Science, Naval Research Laboratory, Washington, DC 20375, USA and Department of Computation and Data Sciences, George Mason University, Fairfax, Virginia 22030, USA

R. S. Crandall
National Renewable Energy Laboratory, Golden, Colorado 80401, USA

B. A. Sperling and J. R. Abelson
Department of Materials Science and Engineering, University of Illinois, Urbana, Illinois 61801, USA
(Received 20 November 2009; revised manuscript received 24 February 2010; published 15 March 2010)

The thermal conductivities of thin films of amorphous Si (a-Si) deposited by hot-wire chemical vapor deposition (HWCVD) are measured by time-domain thermoreflectance (TDTR). Amorphous Si samples prepared at the National Renewable Energy Laboratory (NREL) show an anomalous enhancement in thermal conductivity compared to other forms of a-Si and compared to the prediction of the model of the minimum thermal conductivity. The thermal conductivity of the NREL HWCVD a-Si samples also decreases with increasing frequency of the temperature fields used in the experiment. This frequency dependence of the thermal conductivity is nearly identical to the results of our previous studies of crystalline semiconductor alloys; a comparison of the frequency dependence to a phonon-scattering model suggests that Rayleigh-type scattering controls the mean-free path of ~5 meV phonons in this material. Amorphous Si films prepared at University of Illinois (U. Illinois) do not show an enhanced thermal conductivity even though Raman vibrational spectra of the U. Illinois and NREL samples are nearly identical. Thus, the thermal conductivity of a-Si depends on details of the microstructure that are not revealed by vibrational spectroscopy and measurements by TDTR provide a convenient method of identifying novel microstructures in amorphous materials.

DOI: 10.1103/PhysRevB.81.104203 PACS number(s): 65.60.+a

I. INTRODUCTION

The model of the minimum thermal conductivity is widely used to predict the conductivity of amorphous solids and understand the lower limit of the thermal conductivity that can be produced by generating disorder in crystalline solids.[1] Two recent experiments, however, have demonstrated strong violations of the conventional wisdom: (i) the thermal conductivity of an anisotropic, disordered layered crystal WSe_2 is a factor of five less than predicted by the model;[2] and (ii) the conductivity of a particular form of amorphous Si (a-Si) synthesized by hot-wire chemical vapor deposition (HWCVD) exceeds the predicted value by a factor of 4.[3] The high thermal conductivity of HWCVD a-Si prepared at the National Renewable Energy Laboratory (NREL) is unique: we are not aware of any other amorphous material with a conductivity that so significantly exceeds the predicted value.

The cause of this deviation from the predictions of the model appears to be an anomalously large contribution to heat transport by low-frequency phonons with long mean-free paths. Our initial experiments[3] also indicated that the thermal conductivity measured by time-domain thermoreflectance (TDTR) depends on the modulation frequency of the temperature fields used in the experiment; i.e., the thermal conductivity depends on the spatial extent of the temperature gradient used to determine the thermal conductivity. Previous to these studies of HWCVD a-Si, we have only observed this type of "frequency-dependent thermal conductivity" in crystalline semiconductors alloys such as SiGe and (In,Ga)As.[4] Our interpretation of frequency-dependent thermal conductivity is based on the assumption that thermal conductivity measured by TDTR does not include heat transport by phonons that have mean-free paths larger than the spatial extent of the thermal gradient.[4,5]

Experiments on internal friction at low temperature using high-quality-factor mechanical oscillators showed that HWCVD a-Si prepared at NREL lacks the two-level tunneling states that are characteristic of nearly all other amor-

 ©2010 The American Physical Society

phous solids.[6–8] (In the past year, high-stress amorphous silicon nitride has also been shown to lack two-level systems.[9]) Thus, the HWCVD a-Si films prepared at NREL are unique in three respects: the thermal conductivity is significantly higher than expected; the thermal conductivity is frequency dependent, indicating a significant contribution of phonons with long mean-free paths to the heat transport; and the material lacks two-level systems. In the prior work, however, thermal conductivity data were acquired on a single film of a-Si that was atypical because the film thickness was extremely large, ≈ 80 μm. The purpose of this paper is to report our more extensive measurements and analysis of the thermal conductivity of several NREL a-Si samples as a function of temperature and TDTR modulation frequency. We also characterize the vibrational spectra of the same samples by Raman scattering and make comparisons between the NREL a-Si samples and HWCVD a-Si films prepared at the University of Illinois (U. Illinois).

II. EXPERIMENTAL DETAILS

Amorphous Si films were deposited at the NREL on crystalline Si substrates by hot-wire chemical vapor deposition;[10] the native oxide of the substrates was not removed prior to film growth. The silicon source is SiH_4 gas. Samples H14 and H35 were deposited under the similar conditions that were used to prepare the much thicker layer studied in our previous work;[3] the SiH_4 flow rate was 20 SCCM and the substrate temperature was 425 ± 10 °C. The thicknesses of samples H14 and H35 are 1.6 μm and 2.8 μm, respectively. Growth rates were 0.8 nm/s for H14, 1.0 nm/s for H35, and 2.8 nm/s for the H84 sample that was studied in Ref. 3. The total growth times of samples H14, H34, and H84 were therefore ≈ 30, 50, and 480 min. The internal friction of samples H14 and H35 at low temperatures was previously studied by Liu *et al.*[6]

Samples H1060, H819, and H969 were grown at a lower substrate temperature of 250 °C.[11] The molar ratios of hydrogen gas flow rate to the SiH_4 gas flow rate, an important parameter in determining the hydrogen concentration of samples, were 0, 2, and 4 for samples H1060, H819, and H969, respectively. The hydrogen concentration of H1060 was estimated to be more than 14%, and those of H819 and H969 were 11% and 4%, respectively. Sample H1060 is fully amorphous, sample H819 may contain a small fraction of nanocrystalline regions, and sample H969 is 80% nanocrystalline due to the high hydrogen gas flow rate. Hydrogen dilution is known to produce nanocrystalline growth; the mechanisms that produce nanocrystalline growth are not fully understand but are thought to involve changes in the surface mobility of reactive species or changes in the kinetics of etching reactions.[12] Samples grown with high levels of hydrogen dilution typically show a large volume fraction of nanocrystals when examined by transmission electron microscopy. The thicknesses of the samples are between 1.0 and 1.2 μm. The internal friction of samples H1060, H819, and H969 at low temperature was previously studied by Liu *et al.*[11]

A second set of a-Si films were prepared at the U. Illinois using HWCVD on sapphire substrates. Sapphire was chosen as the substrate to simultaneously provide a high thermal conductivity for the TDTR measurements and large contrast in acoustic impedance so that the longitudinal sound velocity of the a-Si films could be measured by picosecond acoustics. The thickness of the a-Si was measured by spectroscopic ellipsometry. The U. Illinois a-Si films were deposited at substrate temperatures between 114 and 600 °C to explore how the Raman spectra, thermal conductivity, and elastic constants vary with deposition temperature. Substrate temperatures were measured using optical pyrometry. The growth rate of the U. Illinois samples was 0.3 nm/s and the total growth time of each sample was ≈ 10 min.

We used a custom-built spectrometer to measure the Raman spectra. The laser source is an optically pumped frequency-doubled semiconductor laser operating at a wavelength of 488 nm. The power of the laser excitation is typically ≈ 2 mW. Raman-scattered light is collected in a backscattering geometry using a microscope objective with numerical objective of 0.45. Data for the intensity of the Raman scattered light as a function of wavelength are not corrected for variations in the reflectivity of the diffraction grating, the quantum efficiency of the spectrometer charge-coupled-device camera, or the transmission functions of the optical components. (The low-pass optical filter strongly attenuates Raman-scattered light at frequencies below ≈ 130 cm^{-1}.) To facilitate comparisons, we normalize the intensity of the Raman-scattered light by the laser power and the acquisition time. The spectral width of each CCD pixel is ≈ 2 cm^{-1}. With a 488 nm excitation laser, a Raman frequency shift of 100 cm^{-1} corresponds to a wavelength shift of 2.5 nm.

Our system for measurements of TDTR has been thoroughly validated and extensively applied in our studies of the thermal conductivity of thin films,[2,4,5,13] the thermal conductance of interfaces,[14,15] and micron-scale mapping of the thermal conductivity of bulk specimens.[16,17] Techniques for analyzing TDTR data are described in Ref. 18; further details of the sensitivities and uncertainties of the measurements as a function of thermal conductivity, film thickness, and modulation frequency are discussed in Ref. 5. Analysis of the time-domain thermoreflectance data requires as an input the heat capacities per unit volume of the a-Si samples. We have chosen to use the heat capacity of crystalline Si to analyze the data; any systematic errors introduced by this choice are small and comparable to the other uncertainties in the experiment. The heat capacity of a-Si films deposited by e-beam evaporation has been studied by Zink *et al.*;[19] the heat capacity of evaporated a-Si is $12 \pm 2\%$ larger than the heat capacity of crystalline Si in the temperature range $100 < T < 300$ K. Any errors in the heat capacity propagate directly into systematic errors in the thermal conductivity; in other words, if the true heat capacity of HWCVD a-Si is 12% higher than the heat capacity of crystalline Si, then the true thermal conductivity is 12% smaller than the value reported here.

To add to the discussion and further validate the experiments, we also studied the thermal conductivity of a 500-nm-thick layer of a-SiO_2 formed by thermal oxidation of a Si wafer and a bulk substrate of 8 wt % yttria-stabilzed zirconia (YSZ). YSZ is a disordered crystalline oxide with a

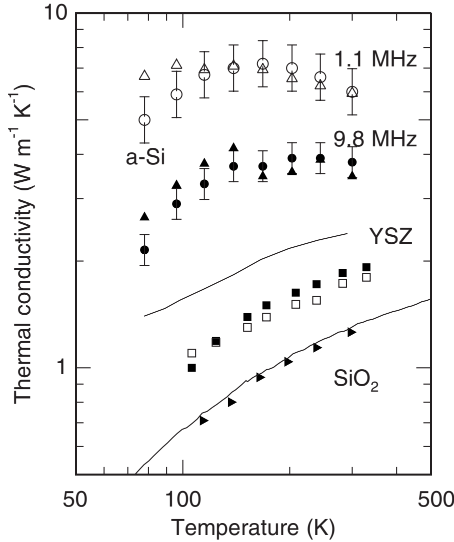

FIG. 1. Temperature dependence of the thermal conductivity of two NREL a-Si films (circles: H14 and triangles: H35) measured with a modulation frequency of $f=1.1$ MHz (open symbols) and $f=9.8$ MHz (filled symbols). Data for cubic YSZ and a-SiO_2 (right-pointing triangles) are included for comparison. Solid lines are the thermal conductivity of YSZ and a-SiO_2 measured previously with the 3ω method, see Ref. 1. Representative error bars of $\pm 10\%$ for $f=9.8$ MHz and $\pm 15\%$ for $f=1.1$ MHz are shown in the data for sample H14.

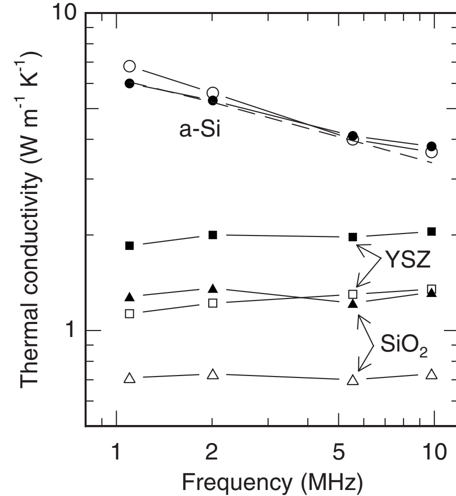

FIG. 2. Thermal conductivity of an NREL a-Si film (H14), YSZ, and SiO_2 as a function of the modulation frequency of the pump beam used in the TDTR measurement. For sample H14 and for SiO_2, the open symbols are for data taken at $T=115$ K and filled symbols are for room temperature. For YSZ, open symbols are for data taken at 154 K and filled symbols are for 328 K. The dashed line shows a theoretical estimate of the frequency dependence based on Eq. (1).

glasslike thermal conductivity that is widely used as a thermal barrier coating.[17]

III. RESULTS AND DISCUSSION

A. Thermal conductivity data

Figure 1 summarizes the principle result of our work: the thermal conductivity for the two NREL HWCVD a-Si thin film samples, H14 and H35, is anomalously high in the temperature range of our measurement, 80–300 K. The thermal conductivity measured at 1.1 MHz modulation frequency is 6.0 W m^{-1} K^{-1} at room temperature, a factor of ≈ 6 larger than the conductivity predicted by the model of the minimum thermal conductivity.[1] The temperature dependence of the thermal conductivity reaches a maximum near 150 K. Both the magnitude and temperature dependence of the thermal conductivity is more reminiscent of semiconductor alloys[20] than typical amorphous solids such as a-SiO_2. Data for YSZ are included in Fig. 1 to emphasize that the conductivity of this unusual form of a-Si can exceed the thermal conductivity of disordered single crystal by a factor of 3. (The thermal conductivity of the sample of YSZ measured by TDTR is $\approx 25\%$ smaller than the conductivity measured by the 3ω method of a similar sample.[1] We do not yet understand the cause of this discrepancy.)

Furthermore, as shown in Figs. 1 and 2, the thermal conductivity of the NREL a-Si samples depends on modulation frequency of the pump beam used in the TDTR experiment. The thermal conductivity of a-Si measured at 9.8 MHz modulation frequency is nearly a factor of two smaller than the conductivity measured at 1.1 MHz at all temperatures; a-SiO_2 and YSZ, on the other hand, do not show a significant frequency dependence larger than the uncertainties in the measurements. The frequency dependence and magnitude of the room temperature data for a-Si, see Fig. 2, is almost identical to what we observed previously in crystalline SiGe alloys.[4]

We have not been able to duplicate the anomalously high thermal conductivity of HWCVD a-Si films grown at NREL in material prepared at U. Illinois. Figure 3 shows how the thermal conductivity and sound velocities vary with the substrate temperature during deposition of the U. Illinois samples; the thermal conductivity increases with deposition temperature but only exceeds 2 W m^{-1} K^{-1} at the highest deposition temperatures. The U. Illinois a-Si films are relatively thin, ≈ 200 nm in thickness; therefore, we could not reliably measure the thermal conductivity of the samples at low modulation frequencies. At 9.8 MHz, however, the thermal penetration depth is smaller than the film thickness and we do not expect that the smaller film thickness of the U. Illinois samples could make a significant difference in the results: for a thermal diffusivity of $D=10^{-2}$ cm^2 s^{-1} and a modulation frequency $f=10$ MHz, $\sqrt{D/(\pi f)} \approx 170$ nm.

B. Analysis of frequency-dependent thermal conductivity

The dependence of the thermal conductivity on the frequency of the temperature fields used in the measurement, see Fig. 2, shows that a significant fraction of heat is carried by phonons with mean-free paths that are comparable to thermal penetration depth. To extract quantitative information from these data requires a model for how the phonon

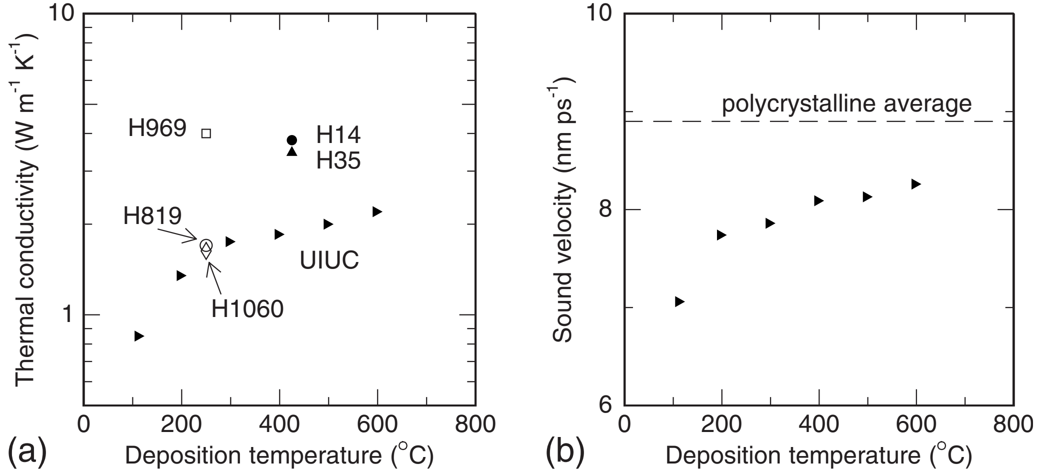

FIG. 3. Variations in the properties of HWCVD a-Si films prepared at U. Illinois (filled right-pointing triangles) as a function of the substrate temperature during film deposition. (a) Thermal conductivity measured at room temperature and (b) longitudinal speed of sound measured at room temperature. Thermal conductivities of NREL samples H1060 (diamond), H969 (open square), H819 (open circle), H14 (filled circle), and H34 (filled up pointing triangle) are included in (a) for comparison. The modulation frequency used to acquire the thermal conductivity in (a) is 9.8 MHz. The uncertainty of the thermal conductivity measurements is $\approx \pm 10\%$. In (b), the dashed line is the averaged longitudinal speed of sound for polycrystalline Si.

lifetimes vary with frequency. For glasses and amorphous semiconductors at low frequencies, inverse quadratic or quartic dependencies are most often considered. The former can arise from either elastic scattering in the few millielectron volts region of the spectrum or from anharmonicity in the much lower-frequency part. The inverse quartic dependence is also often assumed as it represents Rayleigh scattering, although it yields a divergent result for an infinite harmonic solid.

In this section, we provide numerical results, appropriate to our experiment, for a quartic relation between scattering rate, $1/\tau$, and phonon frequency, ω, i.e., $1/\tau = a\omega^4$. Further, we assume that this relation can be used with the same value of the coefficient a, for both transverse and longitudinal branches. (We use sound velocities computed, within the tight-binding electronic structure method, from Fourier transforms of normal modes of a 1000 atom model amorphous structure.) To obtain the contribution to the thermal conductivity for a fixed upper limit of mean-free path, we evaluate a Debye-type expression,

$$\Lambda' = \frac{1}{3\pi^2 v_t} k_B \int_{\hbar\omega_{\mathrm{min},t}}^{10\ \mathrm{meV}} \omega^2 \tau_t(\omega) d\omega + \frac{1}{6\pi^2 v_l} k_B \int_{\hbar\omega_{\mathrm{min},l}}^{10\ \mathrm{meV}} \omega^2 \tau_l(\omega) d\omega, \quad (1)$$

where the prime refers to the fact that this expression is not the total thermal conductivity. In this expression $\tau_i(\omega_{\mathrm{min},i}) = d/v_i$, where d is calculated according to $d = \sqrt{D/(\pi f)}$ using the experimental thermal diffusivity D, f is the modulation frequency of the pump beam, and i denotes the mode polarization, transverse or longitudinal. (For the contribution from $\hbar\omega > 10$ meV vibrational states we rely on our previous Kubo calculations.[3]) The method is not self-consistent because the experimental thermal diffusivity defines the longest mean-free path, which in turn yields the theoretical thermal conductivity which may differ from the experimental value. The value of the coefficient a is adjusted to yield good agreement for the frequency dependence of the thermal conductivity. We find $a = 0.173 \times 10^{-41}\ \mathrm{s}^3$. The result of this calculation ($T = 300$ K) is shown as the dashed line in Fig. 2.

As we have emphasized before the Kubo results cannot be reasonably extrapolated to yield such high thermal conductivities as we observe.[3] Finally, it is important to remark that unless one believes that the thermal conductivity has reached a saturation value at the lowest modulation frequency of the experiment the temperature dependence as shown is deceptive, because within our theoretical model, the higher values of thermal conductivity for the lower temperature arise solely from the difference in d between $T = 300$ K and $T = 115$ K at a fixed modulation frequency.

C. Sound velocities

The longitudinal sound velocities of the U. Illinois samples increases smoothly with increasing deposition temperature, see Fig. 3(b). (We could not determine the speed of sound of the NREL samples because the difference in acoustic impedance between the crystalline Si substrate and the amorphous Si film is too small to produce a measurable echo in the picosecond acoustics experiment.) At deposition temperatures above 200 °C, the longitudinal sound velocity of a-Si approaches 8.3 km s^{-1}, within $\approx 10\%$ of the orientationally averaged sound velocity in crystalline Si, see Fig. 3(b).

We can make a similar comparison between the theoretical predictions of the speeds of sound of crystalline and amorphous Si based, in part, on the models and tight-binding method used for the Kubo calculation of thermal conductivity. The crystalline elastic constants reported in Ref. 21 yield a Voight averaged longitudinal sound velocity of

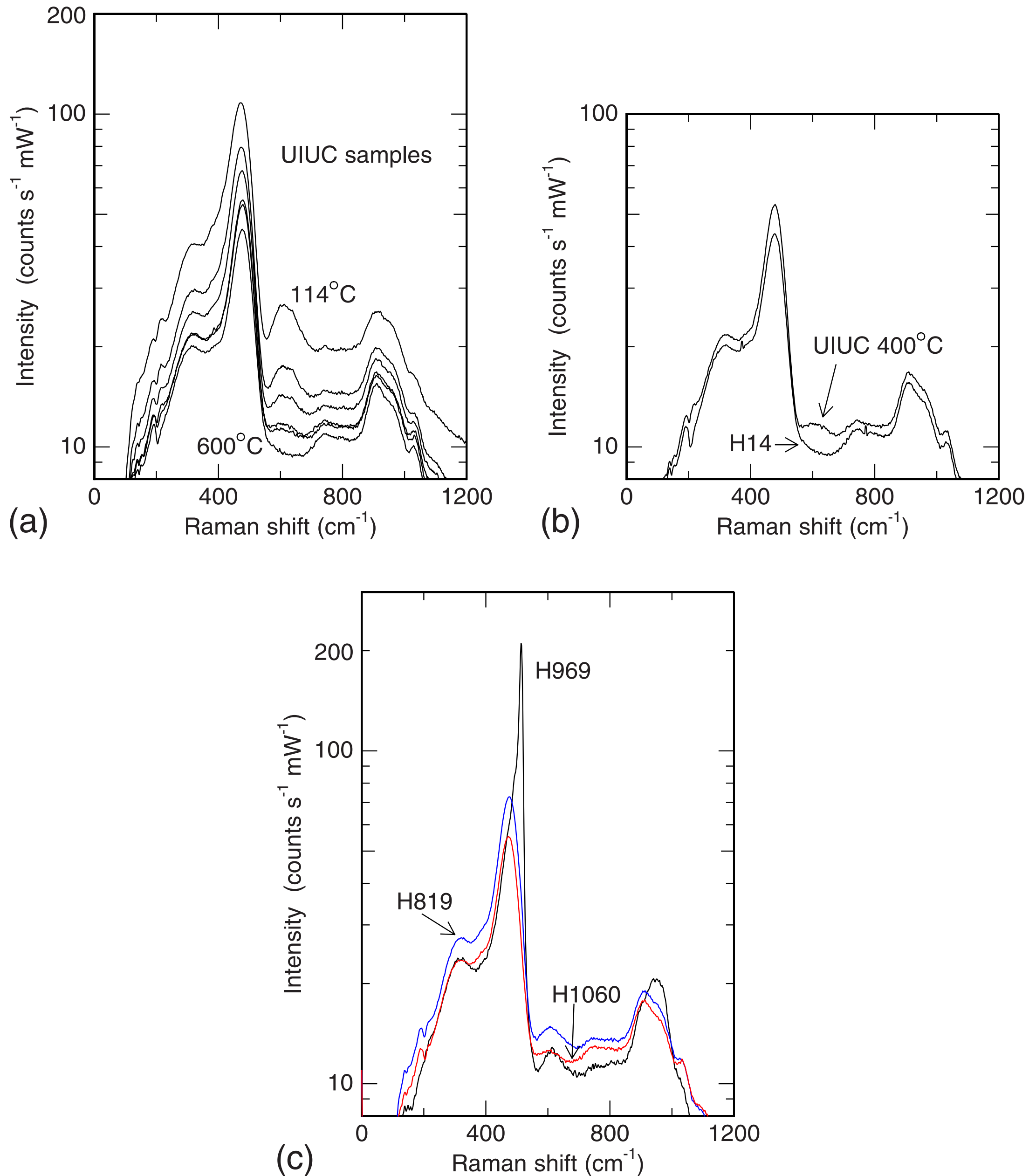

FIG. 4. (Color online) (a) Raman spectra of U. Illinois a-Si films deposited at different substrate temperatures; from top to bottom, the curves are for growth temperatures of 114, 200, 300, 400, 500, and 600 °C. The spectra were collected at room temperature with 488 nm excitation. The overall peak height increases gradually; a broad peak at 615 cm^{-1} appears as the growth temperature decreases. (b) Raman spectra of NREL a-Si film H14 compared to the U. Illinois a-Si film grown at 400 °C. Data for sample H35 (not shown) are indistinguishable from data for sample H14. (c) Raman spectra of NREL a-Si films H1060 (red), H819 (blue), and H969 (black). Raman spectra of H1060 and H819 are similar to the spectra for H14 and H35 except for a weak peak near 615 cm^{-1}. Sample H969 (80% nanocrystalline a-Si) shows a narrow peak at 513 cm^{-1}.

9.56 $km\ s^{-1}$, ≈6% larger than the experimental value. In the calculations described in Ref. 3, we also obtained the longitudinal sound velocities of 1000 atom amorphous structures by considering polarization-projected dynamical structure factors for low Q. The most ordered of these models of the amorphous structure yielded the highest sound velocities with the largest velocity being 7.9 $km\ s^{-1}$, ≈20% lower than the calculated average sound velocity in crystalline silicon.

D. Raman spectroscopy

Raman spectra for these samples, see Fig. 4(a), indicate that the U. Illinois samples are fully amorphous even at the highest deposition temperatures we explored in this work. The Raman spectra of a-Si has been extensively studied: the dominant feature is a broad peak centered near 450 cm^{-1} that arises from a broadened, lower frequency version of the optical phonon near zone center that is the only one-phonon

Raman-active mode in crystalline Si. The shoulder near 300 cm^{-1} and the peak near 900 cm^{-1} are reminiscent of the two-phonon spectra in crystalline silicon that arise from the zone boundary acoustic and optical phonons, respectively. The weak peak below 200 cm^{-1} is the TA-like band.[22] Changes in the deposition temperature produce only small changes in the Raman spectra: a small peak near 220 cm^{-1} appears at high deposition temperatures and a broad peak centered at 615 cm^{-1} that disappears at the highest growth temperature of 600 °C. The broad peak near 615 cm^{-1} has been associated with "wagging" vibrations of Si-H bonds.[23] The disappearance of this spectral feature is consistent with the expected reduction in hydrogen content at high deposition temperatures. We also observe a strong correlation between the intensity at 615 cm^{-1} and the intensity of a peak in the Raman spectra near 2000 cm^{-1} (data not shown) that is characteristic of the Si-H stretching vibration.

HWCVD a-Si grown at NREL has been extensively characterized and we have little doubt that the samples are truly amorphous. This conclusion is reinforced by the Raman spectra acquired on the same samples that were used for the thermal conductivity measurements, see Fig. 4. Figure 4(b) compares the Raman spectra of NREL samples H14 (grown at 425 °C) with the spectra of the U. Illinois a-Si sample grown at 400 °C. (Raman spectra of samples H14 and H35 are indistinguishable.) The main difference in the spectra of the NREL and U. Illinois samples is the presence of the 615 cm^{-1} peak in the U. Illinois sample that we attribute to the Si-H wagging vibration.[23] This suggests that growth conditions at U. Illinois produce, for unknown reasons, significantly higher hydrogen content than the growth conditions at NREL.

The short optical penetration depth $\alpha^{-1} < 30$ nm of 488 nm light in a-Si means that the Raman spectra are only sensitive to the near surface regions of the film: if deeper parts of the samples were for some reason nanocrystalline, Raman spectra acquired with 488 nm light would not reveal this fact. To test for this possibility, we also measured samples H14 and H35 using 785 nm light where the optical penetration depth is on the order of 1 μm. We oriented a $\langle 100 \rangle$ direction of the substrate parallel to the polarization of the laser to suppress one-phonon Raman scattering from the crystalline Si substrate. Raman spectra for samples H14 and H35 acquired at 785 nm (data not shown) are similar to data acquired at 488 nm and we can safely exclude the existence of buried layers of nanocrystalline Si.

E. NREL samples deposited with hydrogen dilution

For completeness, we measured the thermal conductivity and Raman spectra of additional samples of NREL HWCVD Si prepared at lower deposition temperature, 250 °C, and varying hydrogen dilutions, see Figs. 3(a) and 4(c). Sample H1060 was deposited without hydrogen dilution and has an estimated hydrogen content of >14%; the thermal conductivity of sample H1010 agrees closely with the U. Illinois samples deposited at similar substrate temperatures and also without hydrogen dilution. Sample H819 was deposited with moderate hydrogen dilution and has a hydrogen content of 11%; the thermal conductivity is essentially unchanged from sample H1010. As expected, at high hydrogen dilution, sample H969, the film becomes nanocrystalline and a sharp peak appears in the Raman spectra near 513 cm^{-1}, a frequency ≈1% lower than the frequency of the Raman-active optical phonon in crystalline Si. The nanocrystalline microstructure produces an increase in thermal conductivity, from 1.7 to 4.0 $W\ m^{-1}\ K^{-1}$.

IV. CONCLUSIONS

The thermal conductivity of amorphous Si prepared by hot-wire chemical vapor deposition at NREL shows a large enhancement in thermal conductivity compared to the prediction of the model of the minimum thermal conductivity. The magnitude, temperature, and frequency dependence of the conductivity more closely resembles the behavior of crystalline semiconductor alloys than the typical behavior of amorphous solids.

We have not been able to reproduce this behavior, however, in a-Si prepared at U. Illinois by nominally the same growth technique. We can only speculate about the cause of this difference although the higher hydrogen content of the U. Illinois samples probably plays an important role.[6,11] Apparently, the anomalously high thermal conductivity of the NREL a-Si samples is produced by a unique microstructure that is a consequence of low hydrogen content and a delicate balance between the complex kinetic factors involved in the process of chemical vapor deposition.[24] Over the past decade, advances in electron microscopy and computational modeling[25] have provided new insights but fundamental understanding of the synthesis-structure-property relations for a-Si is far from complete. Our work suggests that thermal conductivity measurements by time-domain thermoreflectance provide a useful and convenient method for identifying deposition conditions that produce novel types of order in amorphous Si.

ACKNOWLEDGMENTS

This research was supported by the U.S. Department of Energy under Award No. DE-FG02-07ER46459, by Grant No. R01-2006-000-10742-0 from the Korean Science and Engineering Foundation, and the Office of Naval Research. Experiments were carried out in the Laser and Spectroscopy Laboratory of the Materials Research Laboratory at the University of Illinois, which is partially supported by the U.S. Department of Energy under Grants No. DE-FG02-07ER46453 and No. DE-FG02-07ER46471. We thank Y. K. Koh for his help with the TDTR experiments and W. Wang for Raman spectra at 785 nm.

*d-cahill@uiuc.edu

[1] D. G. Cahill, S. K. Watson, and R. O. Pohl, Phys. Rev. B **46**, 6131 (1992).

[2] C. Chiritescu, D. G. Cahill, N. Nguyen, D. Johnson, A. Bodapati, P. Keblinski, and P. Zschack, Science **315**, 351 (2007).

[3] X. Liu, J. L. Feldman, D. G. Cahill, R. S. Crandall, N. Bernstein, D. M. Photiadis, M. J. Mehl, and D. A. Papaconstantopoulos, Phys. Rev. Lett. **102**, 035901 (2009).

[4] Y. K. Koh and D. G. Cahill, Phys. Rev. B **76**, 075207 (2007).

[5] Y. K. Koh, S. L. Singer, W. Kim, J. M. O. Zide, H. Lu, D. G. Cahill, A. Majumdar, and A. C. Gossard, J. Appl. Phys. **105**, 054303 (2009).

[6] X. Liu, B. E. White, R. O. Pohl, E. Iwanizcko, K. M. Jones, A. H. Mahan, B. N. Nelson, R. S. Crandall, and S. Veprek, Phys. Rev. Lett. **78**, 4418 (1997).

[7] R. S. Crandall, X. Liu, and E. Iwaniczko, J. Non-Cryst. Solids **227-230**, 23 (1998).

[8] X. Liu, R. O. Pohl, and R. S. Crandall, Physica B **280**, 251 (2000).

[9] D. R. Southworth, R. A. Barton, S. S. Verbridge, B. Ilic, A. D. Fefferman, H. G. Craighead, and J. M. Parpia, Phys. Rev. Lett. **102**, 225503 (2009).

[10] A. H. Mahan, J. Carapella, B. P. Nelson, R. S. Crandall, and I. Balberg, J. Appl. Phys. **69**, 6728 (1991).

[11] X. Liu, C. L. Spiel, R. D. Merithew, R. O. Pohl, B. P. Nelson, Q. Wang, and R. S. Crandall, Mater. Sci. Eng., A **442**, 307 (2006).

[12] Subhendu Guha, Jeffrey Yang, Arindam Banerjee, Baojie Yan, and Kenneth Lord, Sol. Energy Mater. Sol. Cells **78**, 329 (2003).

[13] D. G. Cahill, F. Watanabe, A. Rockett, and C. B. Vining, Phys. Rev. B **71**, 235202 (2005).

[14] R. M. Costescu, M. A. Wall, and D. G. Cahill, Phys. Rev. B **67**, 054302 (2003).

[15] H.-K. Lyeo and D. G. Cahill, Phys. Rev. B **73**, 144301 (2006).

[16] S. Huxtable, D. G. Cahill, V. Fauconnier, J. O. White, and J.-C. Zhao, Nature Mater. **3**, 298 (2004).

[17] X. Zheng, D. G. Cahill, and J.-C. Zhao, Adv. Eng. Mater. **7**, 622 (2005).

[18] D. G. Cahill, Rev. Sci. Instrum. **75**, 5119 (2004).

[19] B. L. Zink, R. Pietri, and F. Hellman, Phys. Rev. Lett. **96**, 055902 (2006).

[20] S. T. Huxtable, A. R. Abramson, C.-L. Tien, A. Majumdar, C. LaBounty, X. Fan, G. Zeng, J. E. Bowers, A. Shakouri, and E. T. Croke, Appl. Phys. Lett. **80**, 1737 (2002).

[21] N. Bernstein, M. J. Mehl, D. A. Papaconstantopoulos, N. I. Papanicolaou, M. Z. Bazant, and E. Kaxiras, Phys. Rev. B **62**, 4477 (2000).

[22] M. Marinov and N. Zotov, Phys. Rev. B **55**, 2938 (1997).

[23] M. H. Brodsky, M. Cardona, and J. J. Cuomo, Phys. Rev. B **16**, 3556 (1977).

[24] K. Tonokura and M. Koshi, Curr. Opin. Solid State Mater. Sci. **6**, 479 (2002).

[25] P. Biswas, R. Atta-Fynn, S. Chakraborty, and D. A. Drabold, J. Phys.: Condens. Matter **19**, 455202 (2007).